Finite-size effects on the thermal resistivity of ^{4}He in the quasi-two-dimensional geometry

Chongshan Zhang, Kwangsik Nho, and D. P. Landau
Center for Simulational Physics, The University of Georgia, Athens, Georgia 30602, USA
(Received 2 August 2005; revised manuscript received 6 April 2006; published 11 May 2006)

The thermal resistivity and its scaling function in quasi-two-dimensional (2D) ^{4}He systems are studied by Monte Carlo and spin-dynamics simulations. We use the classical 3D XY model on $L\times L\times H$ lattices with $L\gg H$, applying open boundary conditions along the H direction and periodic boundary conditions along the L directions. A hybrid Monte Carlo algorithm is adopted to efficiently deal with the critical slowing down and to produce initial states for time integration. The fourth-order Suzuki-Trotter decomposition method of exponential operators is used to solve numerically the coupled equations of motion for each spin. The thermal conductivity is calculated by a dynamic current-current correlation function. Our results show that (i) the simulational data collapse onto a single curve for several values of H and temperature, thus supporting the concept of finite-size scaling theory and (ii) the calculated scaling function agrees well with the available experimental results for slabs using two free fitting parameters.

DOI: 10.1103/PhysRevB.73.174508 PACS number(s): 64.60.Ht, 67.40.Kh, 05.10.Ln

I. INTRODUCTION

High-resolution measurements of various properties of ^{4}He confined in restricted geometries near the bulk superfluid transition temperature T_λ have been extensively carried out for over three decades.[1–14] The measurements approach so close to T_λ that the correlation length becomes macroscopic in size. As a result, the whole fluid acts in a correlated way and the values of global properties are changed. This offers an opportunity for testing the finite-size scaling theory, which describes the effect of confinement in a finite geometry near a critical point.

Physical systems which exhibit a second-order phase transition and which are confined in a finite geometry (e.g., a film, a pore, or a box) are thought to be well described by the finite-size scaling theory[15] at temperatures close to the critical temperature T_λ. The finite-size scaling theory is based on the idea that the finite-size effects can be observed when the correlation length ξ becomes of the order of the finite system size (i.e., the side of the cube, the thickness of the film, or the diameter of the pore). For a physical quantity O, this statement can be expressed as follows:[16]

$$\frac{O(\varepsilon,H)}{O(\varepsilon,H=\infty)}=f(x), \tag{1}$$

where

$$\varepsilon=\frac{|T-T_\lambda|}{T_\lambda} \quad \text{and} \quad x=\frac{H}{\xi(\varepsilon,H=\infty)}.$$

Here H denotes the relevant confining length and $\xi(\varepsilon,H=\infty)$ is the correlation length of the bulk system. $f(x)$ is a universal function which does not depend on the microscopic details of the system. It does, however, depend on the observable O, the geometry of the system, and boundary conditions imposed on the system.

Liquid helium ^{4}He has been widely used to examine the validity of the finite-size scaling theory of critical phenomena; sophisticated experimental studies can be carried out in a microgravity environment, for example, Lipa *et al.*[17] measured the specific heat of helium confined in a parallel plate geometry with a spectacular nanokelvin resolution, and the shape of the confining geometry, such as film, pore, and box, can be designed with such a precision that the relevant confining length is well defined.

For superfluid ^{4}He, the scaling of static properties has been studied experimentally, analytically, and numerically. For example, the specific heat near the superfluid transition of ^{4}He has been measured for confinements which vary by a factor of over 1000, and the data to a large extent can be collapsed upon a unique function when properly reduced.[1–4] Field-theoretical calculations for the standard Landau-Ginzburg free energy functional in different geometries with Dirichlet boundary conditions have been carried out[5–7] and the results agree with the specific heat measurements.[8,9] Schultka and Manousakis calculated the superfluid density and the specific heat of ^{4}He in film and pore geometries using Monte-Carlo simulation, and they demonstrated the validity of the finite-size scaling theory.[10–12]

Besides static properties, the finite-size scaling theory can also be understood by studying dynamical properties near the critical point. Among them, the thermal conductivity λ of ^{4}He is a good candidate, because it is a measurable property and its bulk transition has been carefully studied both experimentally[18–20] and theoretically.[21] Murphy *et al.*[22] and Genio *et al.*[23] measured the thermal conductivity of liquid ^{4}He confined in a "microchannel plates" of thickness 2 mm with holes 0.5 and 1 μm in diameter, and their data are consistent with a universal scaling function. Nho and Manousakis[14] studied the thermal conductivity λ of ^{4}He confined in a porelike geometry and the results of their simulations agree well with experiments. Rather recently, Jerebets *et al.* measured the thermal conductivity of liquid ^{4}He confined in a film geometry.[24] In this paper we will study the thermal conductivity λ of confined helium using Monte Carlo and spin-dynamics methods, calculate the scaling function associated with λ for a film geometry, and compare it with the experimental results.

The remainder of the paper is organized as follows: In Sec. II, we will present the model, the simulation methods,

and the method for extracting the thermal conductivity. In Sec. III, we will examine the finite-size scaling theory for the thermal resistivity and compare our calculated scaling function with experimental results. We summarize our results in the last section.

II. MODEL AND SIMULATION METHOD

In this section, we will briefly describe the model and simulation methods used to study the properties of superfluid ^{4}He and show how the thermal conductivity is computed in our model. Matsubara and Matsuda[25] have proposed a lattice model to explain the properties of liquid helium. In the model, the liquid is regarded as a lattice composed of atoms and holes. In terms of operators which create or annihilate an atom at each lattice point, it was proven that the lattice model is equivalent to the spin system. Both systems are classified as model F (or E in the absence of an external field) in the classification of dynamical models and are in the same universality class with the XY model, so we can use the XY model to study the properties of liquid ^{4}He.[26,27]

The Hamiltonian of the XY model on a lattice takes the following form:

$$\mathcal{H} = -J\sum_{\langle ij\rangle}(S_i^x S_j^x + S_i^y S_j^y), \tag{2}$$

where J sets the energy scale, $\langle ij\rangle$ denotes a nearest neighbor pair of spins on a simple lattice in three dimensions, and the summation is over all nearest neighbors. In this model, each spin is a classical spin with three components, $\vec{S}_i = (S_i^x, S_i^y, S_i^z)$.

In our calculations, we use a film geometry, i.e., a $L\times L\times H$ lattice with $L \gg H$, in order to mimic the experiment. Open boundary conditions are imposed along the confining dimension (the H direction). In our model the spins at the open boundary have no neighbors outside the confining space. Periodic boundary conditions are used along the large planar dimensions (L direction), because they better approximate the limit $L\to\infty$.

The thermal conductivity λ of liquid ^{4}He at a given temperature T can be calculated using the dynamic current-current correlation function[28,29]

$$\lambda \propto \int_0^\infty dt \sum_i \langle j_0^z(0) j_i^z(t)\rangle, \tag{3}$$

where the z component j_i^z of the current density $\vec{j}_i$ associated with the lattice point i is defined by

$$j_i^z = J(S_i^y S_{i+e_z}^x - S_i^x S_{i+e_z}^y), \tag{4}$$

where the notation $i+e_z$ denotes the nearest neighbor of the lattice site i in the z lattice direction.

The thermal conductivity calculated from the above equations strongly depends on the initial configuration of the system. The thermal conductivity at a given temperature T is an average value for all possible initial configurations. Therefore, a sequence of uncorrelated equilibrium configurations is needed to provide starting points for the spin dynamics.

These configurations are obtained from a Monte Carlo simulation using the Hamiltonian given by Eq. (2). We use a hybrid Monte Carlo procedure,[28] which consists of ten updates (*MCCMOCMCCO*), where M is a Metropolis update,[30] C is a cluster update[31] and O is an over-relaxation update.[32]

Using this hybrid algorithm, we generate approximately 2000 uncorrelated configurations from the equilibrium canonical ensemble at a given temperature. From each configuration we do dynamic simulations according to the equations of motion for the XY model, which are given as follows:[26,28]

$$\frac{d}{dt}\vec{S}_i = \frac{\partial \mathcal{H}}{\partial \vec{S}_i} \times \vec{S}_i. \tag{5}$$

Starting from a particular initial spin configuration, we perform a numerical integration of these equations of motion using a recently developed decomposition method,[33] which guarantees exact energy conservation and conservation of spin length $|\vec{S}_k| = 1$ and conserves $M_z = \Sigma_i S_i^z$ within its numerical truncation errors. The integration is carried out to a maximum time t_{max} (typically of the order of $t_{max}=200$) with time step $\Delta t = 0.1$ to make sure that we determine the real-time history of every configuration within a sufficiently long interval of time ($0 \le t \le t_{max}$). Fourth-order integrators are used, which are more accurate than a second-order method for the same time step. Finally, we compute the average of a time-dependent observable (such as the current-current correlation function) over all results relative to all the independent initial equilibrium configurations generated via the hybrid Monte Carlo procedure. All error bars for the thermal resistivity correspond to one standard deviation.

III. RESULTS

In this section, we calculate the thermal resistivity, examine its scaling behavior with respect to H, and compare the scaling function with the experimental results. For a film geometry $L\times L\times H$, it is better to keep H finite and let $L\to\infty$ such that the system cannot feel the effect of L for any temperature. In other words, we wish the correlation length to be larger than H, but always less than L for any temperature. We can realize this by performing extrapolation to the infinite limit from the results on finite L. However, we do not have to do this, because we find that by applying periodic boundary conditions along the directions of L, the finite-size effects due to L are already insignificant as long as $L \ge 5H$ (see Fig. 1). Figure 1 shows the thermal resisitivity $R(\varepsilon, H) = 1/\lambda(\varepsilon, H)$ for film lattices as a function of L/H at the critical temperature, where the correlation length is infinite. From Fig. 1, we can see that within error bars, the results of thermal resistivity are the same for $L/H \ge 5$.

Figure 2 shows some of our results of the thermal resistivity $R(T,H)$ as a function of temperature T for various lattice sizes H. The bulk transition temperature $T_\lambda = 1.5518(2)$ is obtained from Monte Carlo simulations.[27] Near T_λ, the data show strong effects of confinement. The smallest size shows the greatest rounding of transition and the thermal resistivity is biggest for the smallest size at the critical temperature. At high temperature, the thermal resis-

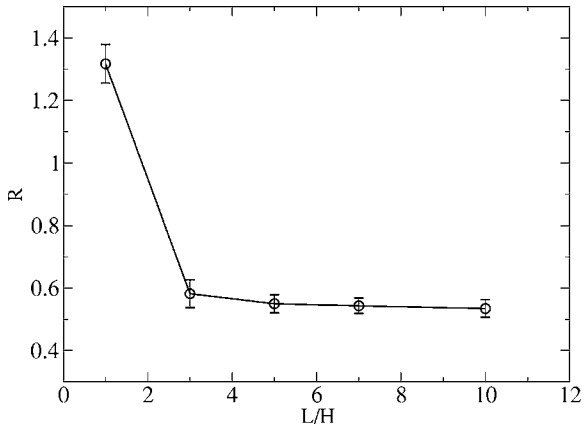

FIG. 1. The thermal resistivity with a fixed $H=6$ at T_λ as a function of L/H.

tivity for different H has no obvious difference within error bars, because $\xi(\varepsilon) < H$.

Now we would like to check the finite-size scaling hypothesis for the thermal resistivity and to compare our results with the existing experimental results.[24] The dependence upon ε of the bulk thermal resistivity can be described by a power law

$$R(\varepsilon) = R_0 \varepsilon^{\chi}, \tag{6}$$

where χ is an effective critical exponent of the thermal resistivity. The dependence upon ε of the correlation length can be described by a power law

$$\xi(\varepsilon) = \xi_0 \varepsilon^{-\nu}, \tag{7}$$

where ν is the critical exponent of the correlation length. Using Eq. (1), the finite-size scaling expression for the thermal resistivity $R(\varepsilon, H)$ is given by

$$R(\varepsilon, H) H^{\chi/\nu} = g(\varepsilon H^{1/\nu}), \tag{8}$$

where $g(x)$ is a universal function.

In this paper, we use the critical exponent of the correlation length $\nu=0.6705$ as determined by Goldner and

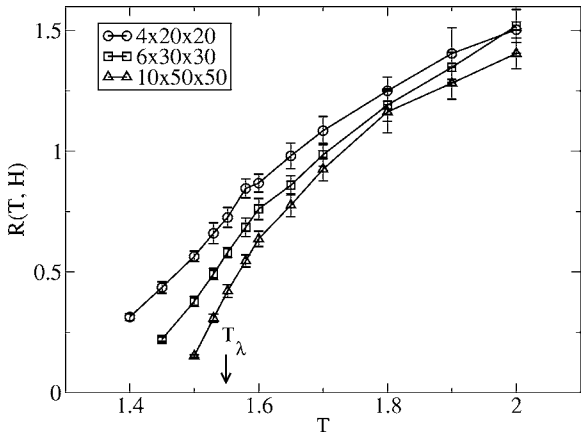

FIG. 2. Thermal resistivity $R(T,H)$ versus temperature for film geometry with sizes that correspond to $H=4$, 6, 10 and $L=5H$. The bulk critical temperature $T_\lambda=1.5518$ is also shown.

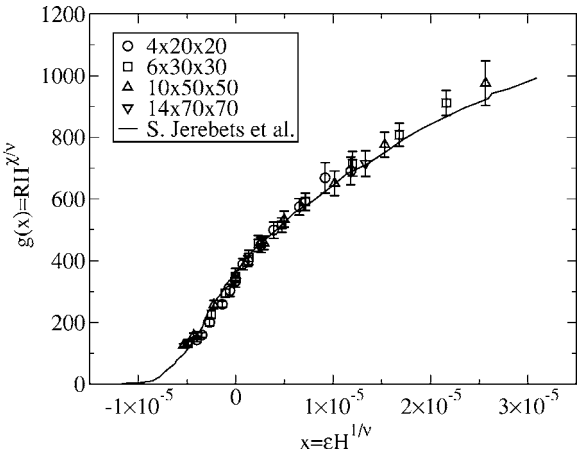

FIG. 3. The universal function $g(x)$ obtained for film geometry. The solid line represents the available experimental results for film geometry (Ref. 24). R is measured in units of cm K/W and H is measured in units of μm. To compare the results of the simulation and experiment, we applied two free-parameter adjustment to the simulation results.

Ahlers.[34] For χ, the dynamic scaling theory[35] predicted an asymptotic value $\chi=\nu/2$. However, Ahlers used the experimental data to determine an effective critical exponent $\chi=0.4397$ at saturated vapor pressure using the power-law fitting [see Eq. (6)] for $3\times10^{-6} \leq \varepsilon \leq 2\times10^{-4}$, and in this fitting, there is no systematical deviation from the power-law fitting, i.e., no need for the correction terms.[36] Furthermore, renormalization group calculations[21] agree with the experimental data of Ahlers, but not with the dynamic scaling prediction. The recent renormalization group calculations[22,37] have yielded results for $\lambda(\varepsilon, H)$, and the slope of the curve of $\log_{10}(\lambda)$ vs $\log_{10}(1/H)$ at $\varepsilon=0$ gives an effective exponent which is very close to the experimental value of Ahlers.

Figure 3 shows a scaling plot of the thermal resistivity scaling function $g(x)=R(\varepsilon,H)H^{\chi/\nu}$ versus the scaled reduced temperature parameter $x=\varepsilon H^{1/\nu}$ with $\chi=0.4397$, where the reduced temperature is taken relative to the bulk transition temperature T_λ. From Fig. 3, we can find that our simulational data collapse onto one single curve for a wide range of values of H and ε, thus supporting the concept of the finite-size scaling theory over a factor of 3.5 in H. However, if we use $\chi=\nu/2$ instead of $\chi=0.4397$, our simulational data are not along one single curve.

The experimental data obtained by Jerebets *et al.* are also shown in Fig. 3 (the solid line). To compare the results of simulation and experiment, we applied two free-parameter adjustments to the simulational data. The two parameter fitting does not change the shape of the scaling function. Figure 3 shows that the agreement between simulation and experiment is quite good except for $x \lesssim -0.4\times10^{-5}$. The difference for $x \lesssim -0.4\times10^{-5}$ may suggest a breakdown of finite-size scaling in the superfluid phase as in the experiment[36] in quasi-one-dimensional.

The geometry is one of the important factors which, in principle, can determine the scaling function. In Fig. 4, we compare the scaling functions for films and pores as determined from computer simulations. From Fig. 4 we can find

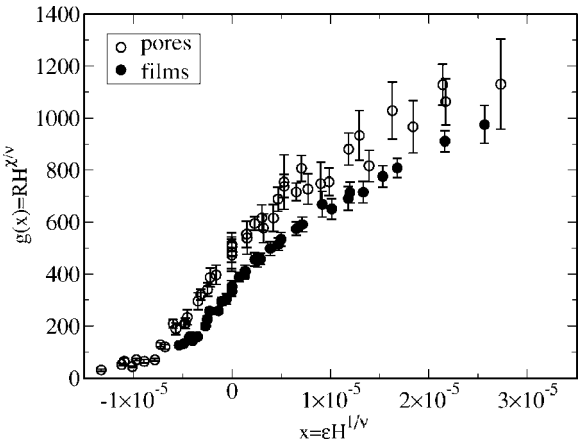

FIG. 4. Comparison of the finite-size scaling functions $g(x)$ for films and pores as determined from computer simulations. The units of R and H are the same as in Fig. 3.

that near T_λ the scaling function for films and pores are different although their shapes are similar. Compared with the scaling function for films, the scaling function for pores shifts to the left, further away from the bulk behavior. This is expected; since in comparison with the film geometry, the pore geometry restricts the dimensionality of the system more, thereby further limiting critical fluctuations. As a consequence, the thermal resistivity for pore geometry is higher at T_λ and decreases to 0 at a lower temperature.

IV. SUMMARY

We have calculated the thermal resistivity $R(\varepsilon,H)$ of liquid ^{4}He in a film geometry (on a $L\times L\times H$ lattice) using the XY model, which belongs to the same universality class as liquid ^{4}He. We applied periodic boundary conditions along L directions and open boundary conditions in the H direction. We obtained the thermal resistivity scaling function $g(x)$ using known values for the critical exponents. We find a good agreement for scaling functions between the results of the simulation and experiment for $x\gtrsim -0.4\times 10^{-5}$ using the temperature scale and the thermal resistivity scale as free parameters. We also compared our calculated scaling function for a film geometry with that for a pore geometry and found a systematic shift.

ACKNOWLEDGMENTS

We thank G. Ahlers for helpful comments and suggestions. This work was supported by NASA under Grant No. NNC04GB24G.

[1] S. Mehta and F. M. Gasparini, Phys. Rev. Lett. **78**, 2596 (1997).
[2] S. Mehta, M. O. Kimball, and F. M. Gasparini, J. Low Temp. Phys. **114**, 467 (1999).
[3] M. O. Kimball, S. Mehta, and F. M. Gasparini, J. Low Temp. Phys. **121**, 29 (2000).
[4] J. A. Lipa, D. R. Swanson, J. A. Nissen, Z. K. Geng, P. R. Williamson, D. A. Stricker, T. C. P. Chui, U. E. Isrealsson, and M. Larson, Phys. Rev. Lett. **84**, 4894 (2000).
[5] R. Schmolke, A. Wacker, V. Dohm, and D. Frank, Physica B **165-166**, 575 (1990); V. Dohm, Phys. Scr., T **T49**, 46 (1993).
[6] P. Sutter and V. Dohm, Physica B **194B-196B**, 613 (1994); W. Huhn and V. Dohm, Phys. Rev. Lett. **61**, 1368 (1988).
[7] M. Krech and S. Dietrich, Phys. Rev. A **46**, 1886 (1992); **46**, 1922 (1992).
[8] J. A. Nissen, T. C. P. Chui, and J. A. Lipa, J. Low Temp. Phys. **92**, 353 (1993); Physica B **194B-196B**, 615 (1994).
[9] A. Wacher and V. Dohm, Physica B **194B-196B**, 611 (1994).
[10] N. Schultka and E. Manousakis, Physica B **194-196**, 537 (1994).
[11] N. Schultka and E. Manousakis, Phys. Rev. Lett. **75**, 2710 (1995).
[12] N. Schultka and E. Manousakis, Phys. Rev. B **52**, 7528 (1995).
[13] A. M. Kahn and G. Ahlers, Phys. Rev. Lett. **74**, 944 (1995).
[14] K. Nho and E. Manousakis, Phys. Rev. B **64**, 144513 (2001).
[15] M. E. Fisher and M. N. Barber, Phys. Rev. Lett. **28**, 1516 (1972); M. E. Fisher, Rev. Mod. Phys. **46**, 597 (1974).
[16] E. Brezin, J. Phys. (Paris) **43**, 15 (1982).
[17] J. A. Lipa, D. R. Swanson, J. A. Nissen, Z. K. Geng, P. R. Williamson, D. A. Stricker, T. C. P. Chui, U. E. Isrealsson, and M. Larsen, Phys. Rev. Lett. **84**, 4894 (2000); J. Low Temp. Phys. **113**, 849 (1998).
[18] W. Y. Tam and G. Ahlers, Phys. Rev. B **32**, 5932 (1985).
[19] M. D. F. Zhong and H. Meyer, J. Low Temp. Phys. **65**, 185 (1986).
[20] W. Y. Tam and G. Ahlers, Phys. Rev. B **33**, 183 (1986).
[21] B. I. Hohenberg and E. D. Siggia, Phys. Rev. Lett. **32**, 1289 (1974); Phys. Rev. B **13**, 1299 (1976); E. D. Siggia, *ibid.* **13**, 3218 (1976); C. DeDominicis and L. Peliti, Phys. Rev. Lett. **38**, 505 (1977); Phys. Rev. B **18**, 353 (1978); V. Dohm, Z. Phys. B **31**, 327 (1978); R. A. Ferrell and J. K. Bhattacharjee, Phys. Rev. Lett. **42**, 1638 (1979); J. Low Temp. Phys. **36**, 165 (1979); P. C. Hohenberg, B. I. Halperin, and D. R. Nelson, Phys. Rev. B **22**, 2373 (1980); V. Dohm and R. Folk, Z. Phys. B: Condens. Matter **40**, 79 (1980); Phys. Rev. Lett. **46**, 349 (1981); G. Ahlers, P. C. Hohenberg, and A. Kornblit, *ibid.* **46**, 493 (1981); Phys. Rev. B **25**, 3136 (1982); V. Dohm and R. Folk, Z. Phys. B: Condens. Matter **45**, 129 (1981); V. Dohm, Phys. Rev. B **44**, 2697 (1991).
[22] D. Murphy, E. Genio, G. Ahlers, F. C. Liu, and Y. M. Liu, Phys. Rev. Lett. **90**, 025301 (2003).
[23] E. Genio, D. Murphy, G. Ahlers, F. C. Liu, and Y. M. Liu, Adv. Space Res. **35**, 87 (2005).
[24] S. Jerebets, Y. M. Liu, F. C. Liu, and G. Ahlers (private communication).
[25] T. Matsubara and H. Matsuda, Prog. Theor. Phys. **16**, 416 (1956); **16**, 569 (1956); **17**, 19 (1957).
[26] P. C. Hohenberg and B. I. Halperin, Rev. Mod. Phys. **49**, 435 (1977).
[27] K. Nho and E. Manousakis, Phys. Rev. B **59**, 11575 (1999).
[28] M. Krech and D. P. Landau, Phys. Rev. B **60**, 3375 (1999).
[29] N. A. Lurie, D. L. Huber, and M. Blume, Phys. Rev. B **9**, 2171 (1974).

[30] N. Metropolis, A. W. Rosenbluth, M. N. Rosenbluth, A. M. Teller, and E. Teller, J. Chem. Phys. **21**, 1087 (1953).
[31] U. Wolff, Phys. Rev. Lett. **62**, 361 (1989).
[32] F. R. Brown and T. J. Woch, Phys. Rev. Lett. **58**, 2394 (1987).
[33] J. Frank, W. Huang, and B. Leimkuhler, J. Comput. Phys. **133**, 160 (1997).
[34] L. S. Goldner and G. Ahlers, Phys. Rev. B **45**, 13129 (1992).
[35] R. A. Ferrell, N. Menyhard, H. Schmidt, F. Schwabl, and P. Szepfalusy, Phys. Rev. Lett. **18**, 891 (1967).
[36] G. Ahlers, J. Low Temp. Phys. **115**, 143 (1999).
[37] M. Topler and V. Dohm, cond-mat/0212277 (unpublished).